

Electrically assisted self-confinement and waveguiding in planar nematic liquid crystal cells

M. Peccianti, A. De Rossi, and G. Assanto^{a)}

National Institute for the Physics of Matter and Department of Electronic Engineering, Terza University of Rome, Via della Vasca Navale 84, 00146 Rome, Italy

A. De Luca and C. Umeton

National Institute of the Physics of Matter and Department of Physics, University of Calabria, 87036 Rende (CS), Italy

I. C. Khoo

Department of Electrical Engineering, Pennsylvania State University, University Park, Pennsylvania 16802

(Received 15 February 2000; accepted for publication 8 May 2000)

We report on spatial soliton formation and self/cross waveguiding in planar cells containing a nematic liquid crystal in the presence of an externally applied voltage. Self-confinement and cross-induced guidance are demonstrated with an Argon ion laser (514 nm) and a helium–neon probe (633 nm), respectively, over millimeter lengths and with milliwatt pump powers. © 2000 American Institute of Physics. [S0003-6951(00)01427-3]

Spatial solitary waves or solitons have been investigated in a variety of configurations and material systems because of their fundamental interest and potential applications in all optically reconfigurable interconnects and light-controlled switching.^{1,2} Very recently, after the pioneering work by Braun *et al.*,³ spatial self-confinement has been experimentally investigated in nematic liquid crystals (NLC) by Warengem *et al.* in capillaries filled with dye-doped NLC,⁴ and by Karpierz *et al.* in planar cells with homeotropically aligned NLC.⁵ Such attention to NLC stems from their large (10^9 times greater than in CS₂) and polarization dependent nonlinearity which, reorientational in nature,⁶ allows the observation of a rich phenomenology despite the relatively slow response.⁷ In experiments for the observation of self-focusing and spatial solitons in NLC, significant attention has been devoted to (a) reduce thermal contributions to the nonlinear phenomena and (b) lower the required optical power. To such extents, while external cooling was employed in Ref. 3 in the presence of excitations as high as 10 W, dye doping was used in Ref. 4 to further enhance the nonlinear optical response, while a hybrid field polarization was launched in homeotropic NLC cells in Ref. 5. In all cases, nevertheless, self-confinement was observed over short distances (hundreds of micrometers) and with nonnegligible thermo-optic effects.

In this letter we undertake an approach towards the observation of spatial solitons in planar NLC cells, applying an external voltage to eliminate the threshold inherent to the Fréedericks transition and defining an input interface to control the field polarization. The latter was aimed at ensuring experimental repeatability while providing a nonpolarized input beam; the former allowed an initial nonzero tilt of the molecular directors with respect to the propagation wavevector, thereby permitting strong reorientational effects at intensities < 50 W/cm.^{5,7,8} In such a configuration, we have

observed diffractionless propagation of an Ar-ion beam over millimeter distances with milliwatt powers, as well as the all-optical formation of a channel guiding a weak He–Ne probe.

The NLC can be modeled as a birefringent medium with orientation locally described by a unit vector or *director*, the spatial distribution of which is governed by elastic forces. When a linearly polarized optical beam propagates in an NLC with a positive optical anisotropy it determines a torque which tends to realign the director parallel to the electric field. Assuming equal Frank constants K for splay, bend, and twist of the molecules,^{6,7} a beam of slowly-varying amplitude A propagating along z , and directors rotating in the plane $x-z$ defined by the optic axis and the electric field vector, the tilt $\hat{\theta} = \theta(A) - \theta_{\text{rest}}$ with respect to the director orientation profile at rest θ_{rest} is described by the elliptic equation

$$4K \left[\frac{\partial^2 \hat{\theta}}{\partial x^2} + \frac{\partial^2 \hat{\theta}}{\partial y^2} \right] + \epsilon_0 \epsilon_a |A|^2 \sin 2(\hat{\theta} + \theta_{\text{rest}}) = 0, \quad (1)$$

with $\epsilon_a = n_e^2 - n_o^2$ the birefringence. The rest distribution in the presence of a low-frequency electric field and in the narrow region traversed by the optical beam can be modeled heuristically by

$$\theta_{\text{rest}}(z, V) = \theta_0(V) + [\theta_{\text{in}} - \theta_0(V)] \exp(-z/\bar{z}), \quad (2)$$

with $\theta_0(V)$ the orientation distribution due to applied voltage far from the input interface, θ_{in} the director orientation at the boundary $z=0$, and \bar{z} a relaxation distance. Finally, the beam amplitude will obey^{7,9}

$$2ik \frac{\partial A}{\partial z} + \left[\frac{\partial^2 A}{\partial x^2} + \frac{\partial^2 A}{\partial y^2} \right] + k_0^2 \epsilon_a (\sin^2 \theta - \sin^2 \theta_{\text{rest}}) A = 0, \quad (3)$$

with $k = k_0 \sqrt{n_o^2 + \epsilon_a \sin^2 \theta_{\text{rest}}}$ the wave vector. For simplicity, we assumed $k \approx k_0 \sqrt{n_o^2 + \epsilon_a \sin^2 \theta_o}$.

^{a)}Electronic mail: assanto@ele.uniroma3.it

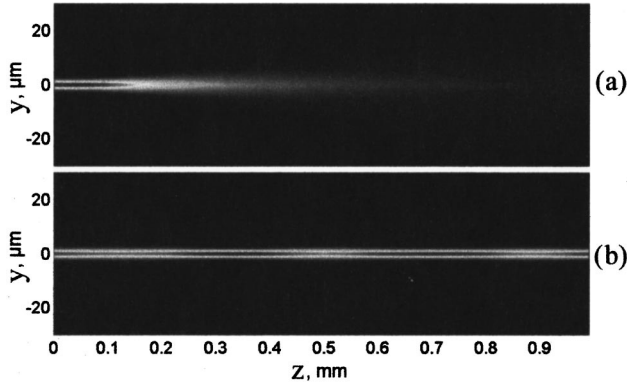


FIG. 1. Contour maps corresponding to numerical simulations from models (1)–(3), with $\lambda=514$ nm, waist= $3\ \mu\text{m}$, $\bar{z}\cong 40\ \mu\text{m}$, input power 3.9 mW, $K=7\times 10^{-7}$ g cm/s², $\epsilon_a=0.2$, and (a) no bias, i.e., $\theta_0=0$, with bias, i.e., $\theta_0=\pi/4$.

θ_0 is zero without ac bias (i.e., planar alignment) and saturates to $\pi/2$ as the bias is increased beyond a few volts for a NLC thickness of the order of $100\ \mu\text{m}$.⁷ The approximations and models (1)–(3) above are valid provided the optically induced reorientation is small and the optical beam propagates in a narrow region, far from top and bottom cell boundaries. In fact, considering a Kerr-like intensity dependent refractive index with a $\sin^2 2\theta_0$ dependence,^{7,8} for $\theta_0 \ll \pi/2$ the self-focusing power P_{sf} is much lower than required by the Fréedericks transition P_F , with^{6,9}

$$P_{\text{sf}} = \pi^2 P_F / 2 \epsilon_a k^2 \sin^2 2\theta_0. \quad (4)$$

Integrating Eqs. (1)–(3) with $\theta_{\text{in}} = \pi/2$, we verified the consistency of the model and were able to compare the system behavior in the absence [Fig. 1(a)] and in the presence [Fig. 1(b)] of the external bias ($\theta_0 = \pi/4$) for a linearly x -polarized Gaussian input beam with a power of 3.9 mW and a waist of $3\ \mu\text{m}$. The formation and propagation of a self-confined solitary wave is apparent in the contour map of Fig. 1(b).

To demonstrate the self-confinement, we employed a planar glass cell with mylar spacers, indium–tin–oxide electrodes and silicon–oxide films at the glass–NLC interfaces (Fig. 2). The former allowed the application of an ac (1 kHz) voltage across the $75\ \mu\text{m}$ thick crystal, while the latter ensured the planar alignment of the NLC directors. Another

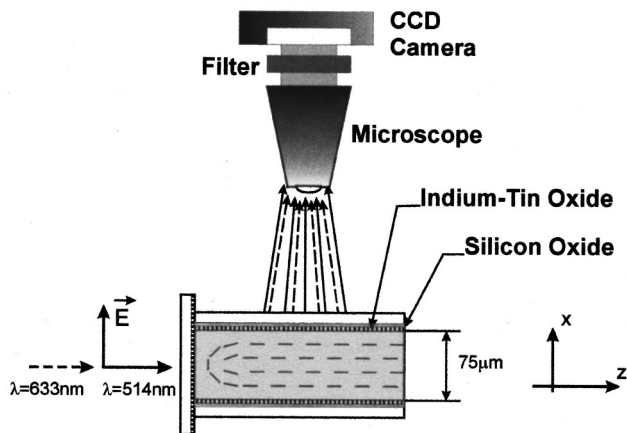


FIG. 2. Sketch of the experiment. The cell is properly oriented with an x – y – z – θ stage, and the input beam(s) collimated (along z) and linearly polarized.

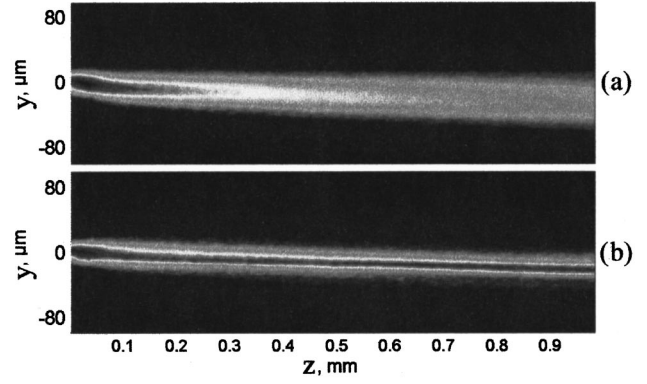


FIG. 3. CCD acquired images of the light scattered from the x -polarized Ar^+ beam in the cell, (a) with no external bias, and (b) 40 s after applying a bias of 0.8 V at 1 kHz across the $75\ \mu\text{m}$ thick cell. The input power was 4.2 mW in both cases.

pretreated glass slide was used to define the input boundary $\theta_{\text{in}} = \pi/2$ in $z=0$ and, therefore, keep the light polarized along x . The cell was then filled up with the nematic ‘‘E7’’ allowing light propagation over centimeter distances. A 514 nm beam from an Ar-ion laser was collimated to a waist $\leq 2.5\ \mu\text{m}$ using a $20\times$ microscope objective and launched in the cell, well removed from bottom and top glass boundaries. A microscope and a charge coupled device (CCD) camera allowed us to collect the light scattered above the cell and investigate the beam evolution in the y – z plane, as sketched in Fig. 2. If the absence of bias, the beam diffracted as in Fig. 3(a), which is the image collected for an input power of 4.2 mW. By analyzing the scattered light and its polarization we could estimate a $\bar{z} \cong 50\ \mu\text{m}$, propagation losses of $5\ \text{cm}^{-1}$ and a divergence of nearly 5° , i.e., a Rayleigh distance close to $55\ \mu\text{m}$. Within 30–40 s after the application of a 0.8 V (root mean square) bias, however, after the initial rearrangement at the interface ($z=0$ – $50\ \mu\text{m}$) the beam self-confined and propagated in a diffractionless fashion, as shown in Fig. 3(b). This behavior is, within experimental errors, a clear indication of a three-dimensional (3D) spatial soliton. It propagated with an unchanged waist over 20 times the diffraction length, covering distances in excess of 1.4 mm and essentially limited by the losses. To verify the reorientational nature of the nonlinearity, as used in models (1)–(3) above, we repeated the experiments at diffraction input polarizations, with and without bias. The results were always consistent with the model and confirmed our interpretation. When the power was raised to compensate for a smaller bias or a nonideal x -polarized input, however, thermal effects and/or strong self-focusing occurred, resulting in instabilities and beam breakups. Similarly, strongly focused or diverging input beams led to uncompensated diffraction/lensing in the cell, as we will discuss in detail elsewhere. Finally, larger biases well above 1.5 V reduced the response time of the NLC cell but also caused the saturation of the director reorientation, thereby impeding the soliton formation.

To further ascertain the nature of the effect, we also co-launched a weak collinear He–Ne probe at $\lambda=633$ nm and verified that it was guided by the soliton only if copolarized with it, demonstrating the nonthermal origin of the nonlinear response. The He–Ne propagation corresponding to the two cases in Fig. 3 was studied with an additional

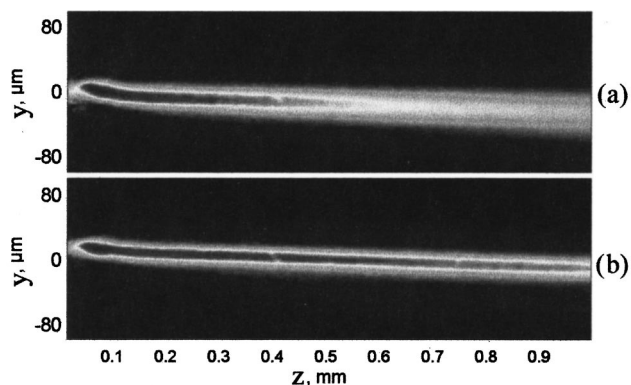


FIG. 4. CCD images of the light scattered from the He-Ne beam ($\lambda=633$ nm) co-launched and co-polarized with the Ar^+ beam (same conditions as in Fig. 3). In (a) the green soliton is not formed (no bias), whereas in (b) the soliton makes a channel supporting the guided-wave propagation of the weak ($30 \mu\text{W}$) probe.

band-pass filter in front of the CCD camera, and the results are shown in Fig. 4. These pump-probe experimental results demonstrate the formation of an all optically induced (polarization sensitive) channel waveguide.

In conclusion, we have demonstrated 3D spatial solitons in electrically-biased planarly-oriented nematic liquid crystals. The observed solitons, at powers of a few milliwatts and for propagation length orders of magnitude longer than the diffraction distance, are due to the reorientational nonlinearity and support the confinement of a copolarized weak signal at a longer wavelength. Furthermore, since the director axis reorientation is a nonresonant effect, the observed phenom-

ena are independent on the wavelength actually employed, and could easily be reproduced in the $1.3\text{--}1.5 \mu\text{m}$ spectral regions of relevance for optical communications, where they have important implications towards all optically reconfigurable interconnects. We are presently extending our work to the near infrared and to partially and totally incoherent light beams.¹⁰

The authors gratefully acknowledge discussions with Dr. M. Karpierz (Tech. Univ., Warsaw, Poland), Dr. N. Tabiryan (Beam Engineering Corp., Oviedo, USA), Professor F. Simoni (Univ. Ancona, Italy), and Professor M. Warengem and his group (Univ. d'Artois, France).

¹M. Segev and G. I. Stegeman, *Phys. Today* **51**, 42 (1998).

²See, for example, *Beam Shaping and Control with Nonlinear Optics*, edited by F. Kajzar and R. Reinisch (Plenum, New York, 1997), B369.

³E. Braun, L. Faucheux, and A. Libchaber, *Phys. Rev. A* **48**, 611 (1993); E. Braun, L. Faucheux, A. Libchaber, D. W. McLaughlin, D. J. Muraki, and M. J. Shelly, *Europhys. Lett.* **23**, 239 (1993).

⁴M. Warengem, J. F. Henninot, and G. Abbate, *Opt. Express* **2**, 483 (1998).

⁵M. A. Karpierz, M. Sierakowski, M. Swillo, and T. Wolinsky, *Mol. Cryst. Liq. Cryst.* **320**, 157 (1998).

⁶N. V. Tabyrian, A. V. Sukhov, and B. Ya. Zel'dovich, *Mol. Cryst. Liq. Cryst.* **136**, 1 (1986).

⁷I. C. Khoo, *Liquid Crystals: Physical Properties and Nonlinear Optical Phenomena* (Wiley, New York, 1995).

⁸R. M. Herman and R. J. Serinko, *Phys. Rev. A* **19**, 1757 (1979).

⁹D. W. McLaughlin, D. J. Muraki, M. J. Shelley, and X. Wang, *Physica D* **97**, 471 (1996).

¹⁰M. Mitchell, Z. Chen, M. Shih, and M. Segev, *Phys. Rev. Lett.* **77**, 490 (1996); M. Mitchell and M. Segev, *Nature (London)* **387**, 880 (1997).